Intelligent Single IMU Sensor Module for Gait Temporal Parameter Estimation

Amit Bhongade, Rohit Gupta, Tapan Kumar Gandhi, Prathosh AP

***Abstract*—Human gait parameters reveal a lot about physical and psychological well-being. In addition, gait impairments significantly affect daily life activities and hamper the locomotive freedom of people with neurological or musculoskeletal disorders. However, there is still a need for a portable, user-friendly, cost-effective gait characterization device. Therefore, in this study, a feature engineering-based portable gait characterization module is proposed, and a shank-mounted inertial measurement unit (IMU) is utilized for gait phases and event detection. The efficiency of the developed module is estimated on ten healthy subjects for plain terrain walking. A force sensing resistor (FSR) sensorized instrumented insole has been utilised as a reference system to validate the results estimated using the developed module. The performance is estimated with three different classifiers, support vector machine (SVM), K-nearest neighbor (KNN), and linear discriminant analysis (LDA). For gait event identifications, the average classification accuracies depicted by SVM, LDA, and KNN classifiers are 95.69±5.23%, 96.64±5.02%, and 93.63±4.84% ($p - value < 0.05$), respectively. Furthermore, the confusion matrix demonstrated the insight illustration of predicted and misclassified events for individual classifiers. In summary, the gait events and gait temporal parameters are reliably estimated using a single IMU with SVM or LDA classifier ($p - value > 0.05$). Additionally, the efficacy of the proposed model for sensor location and subject variability has been evaluated. The performance of LDA and SVM classifier for gait phase prediction has been found invariant ($p - value > 0.05$) towards sensor location and subject variability.**

***Index Terms*—Classification, Embedded system, Gait characterization, Gait-phase prediction, Inertial measurement unit.**

I. Introduction

GAIT analysis plays a vital role in assessing walking activity and irregularity in human walking patterns. Variation in walking patterns provides valuable information about abnormal psychological and physical conditions. Gait analysis finds applications across sports, clinical health diagnostics, and rehabilitation, among others [1]. In clinical health diagnostics, Several approaches have been suggested in the literature., such as a method to perform ambulation monitoring for patients with Parkinson's disease (PD) has been developed and feature engineering techniques have been extensively utilised to discriminate between people with PD and healthy individuals automatically [2]–[7]. Furthermore, an investigation was conducted to develop a technique for differentiating between patients suffering from medial knee osteoarthritis and asymptomatic individuals using gyroscopes and accelerometers [8], [9]. These methods help patients improve their health conditions and quality of life. Similarly, gait analysis can be used in rehabilitation to monitor the patient's recovery from any movement disorder. In medicine and healthcare, gait analysis is an assistive tool and fundamental method to characterize human gait, which enhanced the interest of clinicians and researchers. In sports activities, gait analysis has been implemented to recognize the indiscretions and faults in the athlete's performances in various sports events, such as running and swimming, so that they can analyze and improve [10], [11]. These gait analyses can be used to understand poor biomechanics, avoid future overuse injuries, help athletes achieve high-level performance, and perform high running or jumping. The moment can lead to significant injuries by falling or tripping during running when the foot is in the mid-swing phase. These days gait analysis is limited to laboratory-based settings, but the reality proves that demands for real-life portable monitoring and measurement devices are high [12].

Gait characterization can be done using various techniques, from simple and affordable to highly advanced. For instance, footprint recording while ground walking to identify one's stride is cheap and straightforward. The shoe bottom is painted to accomplish the following so that the impression of the footprint can be observed on the ground. O'Sullivan et al.'s study employed standard walk tests, including the 6-minute and 10-meter walk tests, for gait analysis [13]. The temporal metrics, such as step and stride times, are also measured during the ground walk using a stopwatch. Even so, this method of determining gait is frequently employed in typical settings, although it still has problems with scarce resources and measurement subjectivity [13], [14]. The limitations and challenges in the conventional environment have been resolved with stereophotogrammetric systems [15], walk mats [16], and wearable devices [17]–[22]. The stereophotogrammetric system is a multi-camera motion capture system that provides the instantaneous position of markers that can be used for gait characterization. While these systems excel in gait characterization, they are hindered by their high costs, lengthy setup process, restricted to laboratory-based settings, and operational complexity, which arises from the specialized technical expertise required for operation. Similarly, pressure mats are more dependable and cost-effective than a stereophotogrammetric system for measuring gait, but use is restricted to adequately equipped laboratories and overground gait exercises. These drawbacks motivated researchers to explore wearable and cost-effective solutions for gait characterization.

Gait characterization can be performed using motion, force, goniometers, and piezoelectric sensors. Thus, researchers have started investigating the pressure sensors. The FSR have been utilized for gait characterization, as shown in the study conducted by Beauchet et al. [23]. FSRs placed beneath the feet are utilized to detect gait-related occurrences like toe-off (TO) and heel-strike (HS), enabling the measurement of

spatiotemporal gait parameters. In the literature, researchers presented the significance and use of multiple FSRs (2 to 32 in number) located in different regions of the feet to characterize the gait [24]–[26]. Multiple FSRs improve the accuracy and precision of the measurement because it provides information on all parts of the feet touching the ground, which helps in detecting flat foot and gait abnormality. Nevertheless, it increases the number of data channels that improve the hardware complexity and difficulty identifying and rectifying faulty FSRs, This troubleshooting complexity renders it impractical for real-world application. Furthermore, few FSRs can fail to pick up specific components of gait impairment, such as foot eversion/inversion [27], often observe in post-stroke subjects [28].

In prior research, significant endeavor was dedicated to developing practical and valid alternatives to address the constraints associated with laboratory testing, notably the time-consuming setup and costly equipment [29], [30]. A focused research and development technique has been proposed by the researchers to capture the lower limb motion with the limited expert knowledge required and without expensive equipment [31], [32]. The Inertial Measurement Units (IMU) appeared as a promising device to authorize unobstructed, affordable, daily life detection of gait in a wide abundance of cohabitation [33], ranging from neurological diseases such as somnambulism (sleepwalking), and Parkinson's [34] to Stroke [35]. One benefit of IMU-based gait assessment is the ability to measure walking responses to environmental changes, thereby improving the ecological validity of the testing process [36]. IMU sensor poses several challenges due to drift problem and inherent sensor noise. These challenges limited the widespread use of IMU-based systems for pervasive healthcare [37], [38]. However, many literatures present reliable and efficient ways to estimate gait parameters using feature engineering techniques. In this context, features measured from the IMU signal are utilized for spatiotemporal gait parameters prediction [39], [40]. The study conducted by Hannink et al. utilized deep learning to calculate the stride length and trained the model using a freely available dataset of 101 geriatric patients [41]. The research did not prioritize the assessment of temporal gait metrics. Moreover, deep neural networks are not well suited for real-time embedded applications.

In this study, a single IMU sensor-based system has been developed and its performance validated against an FSR sensor insole [24], [25]. In addition, temporal gait events and phase estimation approaches have been proposed using feature engineering techniques. This approach is fully data-driven and does not depend on assumptions or theoretical models. Furthermore, the gait events (TO, HS) estimation has been performed using gait phase information (swing and stance phases) that is mainly calculated using an IMU sensor signal. The primary objectives of this study are to offer a user-friendly, affordable, machine-learning (ML)-driven, and wearable system for gait characterization. Moreover, the conventional machine learning approach made it more suitable for embedded implementation.

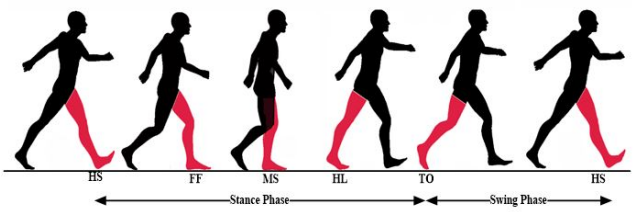

Fig. 1. Gait Phases and Gait Events of a Complete Gait Cycle.

II. MATERIALS AND METHODS

A. Gait Temporal Characterization

Human gait is the linear advancement of the human body's movement generated by synchronized, rotated movements of body parts. Everyone has their gait pattern. The fundamental purpose of gait is to support the HAT (head, arms, trunk), balance the body, and maintain an upright posture. Gait is defined as a balanced, alternating, and cadenced movement of lower limbs that results in the forward progression of the body. A stride represents the single gait cycle (GC), which begins with HSs and ends when the next hHSs the ground of the same leg. The single GC contains a 60% stance phase (STP) and a 40% swing phase (SWP) [33]. The stance phase contains subevents such as HS, heel-lift (HL), mid-stance (MS), flat-foot (FF), and TO. Further, the swing phase is divided into the initial, mid, and terminal swings, as shown in Fig. 1.

Gait temporal parameters include stride time, step time, stance time, and swing time. Furthermore, these parameters are used in identifying gait impairment, assessing, and treating individuals with pathological situations that affect their walking, such as Parkinson's, Stroke, and sleepwalking. Any movement disorder affects the walking of the patients, which could be identified using these parameters. The GC can be subdivided into two phases: one STP and a second SWP. HS of any leg represents the starting of the STP, however, the SWP initiates when TO happens for the same leg. When the TO and HS of the GC are detected then all spatiotemporal parameters are measured. Brief formulas to measure the temporal gait parameters are explained below [42].

Stride Time: It is the duration between two consecutive HSs of same foot and is calculated using the time between HS(i) of one leg and the next HS(i+1) of the same leg.

$$Sride(i) = HS(i+1) - HS(i). \tag{1}$$

Stance Period: It is the time duration between HS and TO of the same leg and calculated using the time between TO(i) and HS(i) of the same leg.

$$Stance(i) = TO(i) - HS(i). \tag{2}$$

Swing Period: This refers to the period during which the foot is completely lifted off the ground, calculated by measuring the time between TO(i) and HS(i+1).

$$Swing(i) = HS(i+1) - TO(i). \tag{3}$$

Step Time: This is the duration between two consecutive foot contacts with the ground of the opposing foot. It is

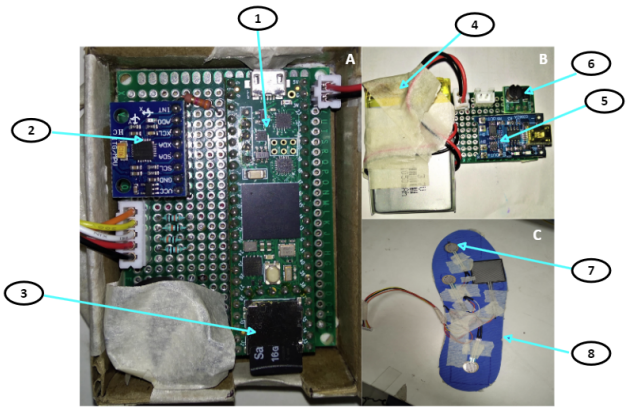

Fig. 2. Developed Hardware Module. (1) Microcontroller; (2) IMU; (3) SD Card; (4) Li-ion battery; (5) battery charging module; (6) DC-DC voltage regulator; (7) FSR Sensor; (8) Insole.

calculated using the time between left leg HS(i) and Right leg HS(i).

$$StepTime(i) = HS_{right}(i) - HS_{left}(i). \quad (4)$$

B. Developed Hardware System

The proposed module consists of four submodules: one 6-DoF IMU sensor, a power supply, instrumented insole with FSR sensors, and the microcontroller, as shown in Fig. 2. The microcontroller has 4K EEPROM (emulated) memory, 1024K RAM, 7936K Flash, ARM Cortex-M7 at 600MHz, 8 serial, 3 SPI, 3 I2C ports, 18 analog input pins, 35 PWM output pins, 55 digital input/output pins, SD Card port, and RTC for date/time. The Arduino IDE software, supplemented with the Teensyduino add-on, serves as the programming environment for this microcontroller. The insole consisted of four FSR sensors [23], one at the toe, one at the heel, and two at the metatarsal region of the foot. The IMU sensor is linked to the microcontroller's Inter-Integrated Circuit (I2C) digital pins. This IMU unit measures a three-axis gyroscope (Gyx, Gyy, and Gyz) with a three-axis accelerometer (Accx, Accy, Accz) to form a standalone six-axis unit. The IMU sensor is mounted in the main module, as depicted in Fig. 2. To perform the data acquisition and detect gait walking patterns, a module is affixed to the shank area of the lower limb, positioned above the ankle. The power consumption when running at full speed of 600 MHz, 100 mA current, and runs on 1.25 V. The battery used has a capacity of 1000 mAh, so the total duration it can run for (1000mAh/100mA) is 10 hours. The output signals from FSR and IMU had a sampling frequency of 100 Hz. Simultaneously, these signals were stored on the data storage module (SD card) in text file.

C. Experimental Setup and Data Acquisition

The developed hardware was used to acquire the signal for walking activity which was further utilized for machine learning model development and gait analysis. A total of ten participants, without any neuromuscular and gait disorder (average height 176.6±6.94 cm, weight 73.2±5.07 kg) aged between 20 to 40 years, voluntarily participated in the experimental sessions. The Indian Institute of Technology (IIT) Delhi Ethics Committee granted approval for the proposed research (Ref no: 2021/P015). The subjects were asked to give written consent before the experiment. The signals acquired during the experiment were purely non-invasive. The signals were acquired using the developed sensor module, which consists of an FSR sensor and an IMU sensor. The sensor module developed was affixed to the shank area of the participants' right foot, specifically at the ankle, as shown in Fig. 3 [43].

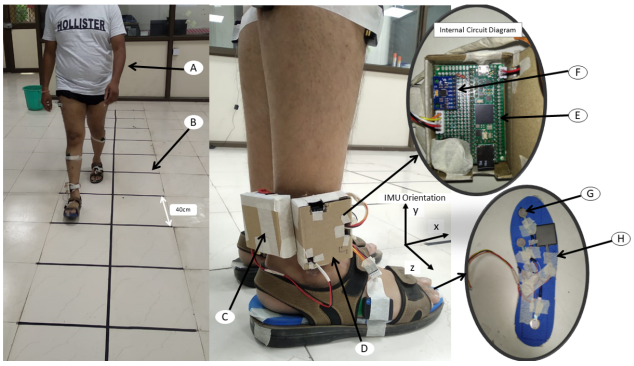

Fig. 3. Experimental Setup and Wearable Device. (A) Participant; (B) Walking Path; (C) Battery Module; (D) Central Module With IMU; (E) Teensy 4.1 Microcontroller with SD Card; (F) IMU Sensor; (G) FSR Sensor; (H) Insole.

The wearable device is sized 7.5 cm x 5.5 cm x 2.5 cm. The inertial sensor is oriented so that the x-axis aligns with the walking direction. The complete experimental setup is depicted in Fig. 3. The laboratory featured a straight path measuring 10 meters in length and 0.8 meters in width, marked with one-sided black tape.

In the experiment, the participants were asked to walk at a self-paced on the experiment pathway. For each subject, a total of ten trials were recorded, further, the subjects were instructed to flex his/her knee with full range of motion, followed by foot tapping, at the start and end of each trial. It was used to synchronize the IMU and FSR signals and to separate the gait trials. The collected data during the experiment was stored in the SD card module of the main system

D. Signal Processing

All the signal processing was implemented with MATLAB R2021b, on a computer with Windows 10, an Intel® Core™ i9-10900K CPU @ 3.70GHz, and 128 GB RAM. The acquired FSR and IMU signal, stored in an SD card, and data was imported to the PC for further analysis. Fig. 4 shows the normalized raw signals of IMU and FSR sensors (heel and toe).

1) Gait Phase (GP) and Gait Events (GE) Detection using FSR: The signal of two FSR sensors (Heel and Toe) was utilized to estimate GPs (STP and SWP), and GEs (HS and TO) and to estimate the gait temporal parameters [24], [25]. Moreover, these values also serve as a reference to estimate the performance of the developed IMU-based gait characterization model. First of all, the walking trials were separated using the IMU sensor signal. Fig. 4 (a, b) shows the recorded IMU signal

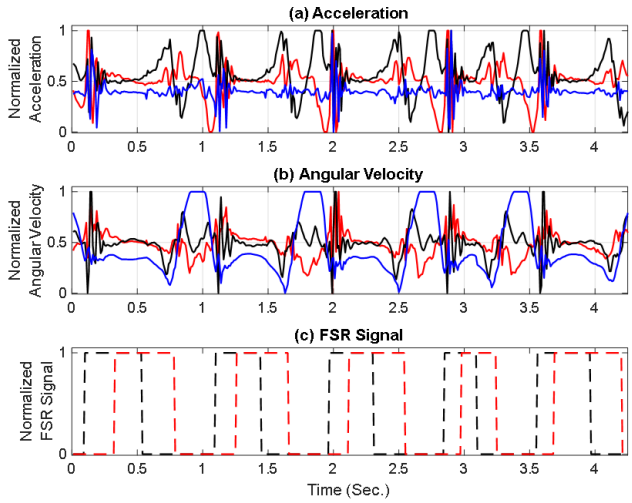

Fig. 4. Normalized raw signals of IMU and FSR sensor ((a-b) X-axis: Black, Y-axis: Red, Z-axis: Blue, (c) Heel FSR: Black dotted and Toe FSR: Red dotted).

of subject 1. As mentioned earlier, the subjects were asked to flex his/her instrumented leg's knee twice at the start and end of each trial. These events are distinctively identified by the z-axis gyroscope (Gyz) signal; hence it was used to separate the individual trials. Further, for every trial, TO and HS events have been identified using the FSR dataset.

Fig. 5 and Fig. 6 show the flow chart and algorithm to detect the GEs and GPs from the FSR signal. At every instance, the designed algorithm looked for the knee flex event (annotating the start of the trial) as soon as it was detected, the algorithm checked for the HS and subsequently for the TO event or the next knee flex event (annotating the end of the trial). The TO and HS events detected in between the trials were used to estimate the gait phase and gait temporal parameters. These temporal gait parameters and gait phases served as reference values for IMU-based model validation.

2) Feature Extraction and Classification Algorithm: Fig. 7 illustrates a block diagram representing the signal processing pipeline employed in the design of the gait characterization module utilizing the IMU signal. All the signals were imported from the SD card to the computer. During the preprocessing stage, the IMU signal from all six degrees of freedom was filtered using a zero-lag, fourth-order Butterworth bandpass filter, with a cutoff frequency range of 0.5 to 10 Hz.

Moreover, filtered data was normalized through the min-max normalization method, which ensures consistency and comparability across different datasets [44]. Additionally, the precise extraction trials from recorded data are a crucial step for the performance of the training model. The trials were extracted using the Gyz signal generated from voluntary knee flexion movement performed at the start and end of the trial. Subsequently, an overlapped windowing algorithm is utilized to segment all the signals (gyroscope, accelerometer) for further processing. For the current study, a window size and window shift of fifteen and one sample were opted, respectively. Further, for each window, six-temporal features were extracted. The extracted features were skewness, variance,

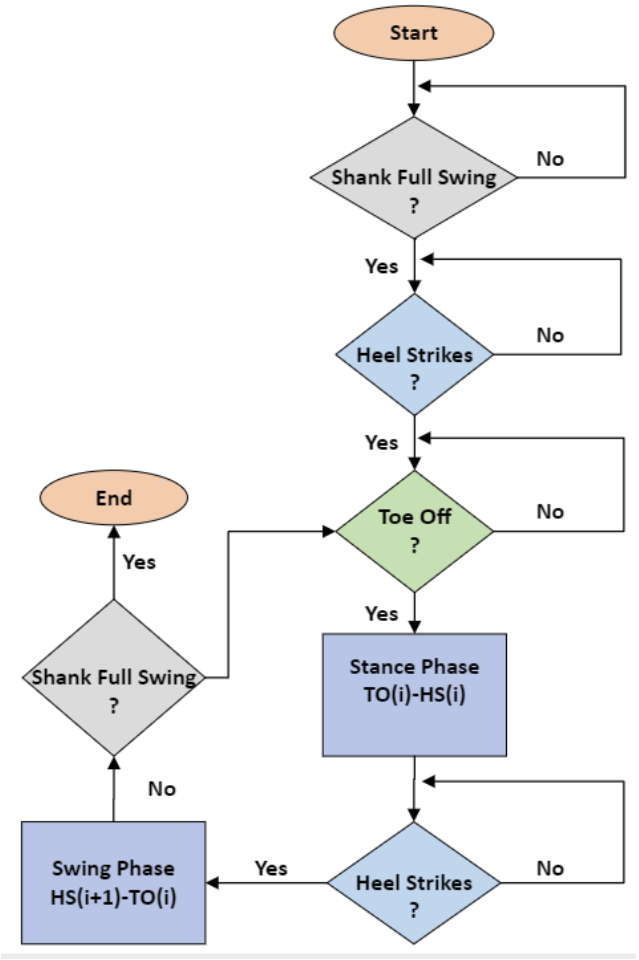

Fig. 5. Flow chart and pseudo code to detect the GEs and GPs from the FSR signal.

root mean square, kurtosis for individual Degree of Freedom, and correlation between each pair of Degree of Freedom of gyroscope and accelerometer [45]. It resulted in a total of 36 features for each feature vector. The feature vector associated with the SWP was designated as '1', while those belonging to the STP were labeled as '2'. The system's performance was assessed using 10-fold cross-validation. In this process, out of ten recorded trials, one trial was reserved for testing the classifier, while the remaining trials were utilized for training. This cross-validation procedure was repeated until each trial underwent testing.

Additionally, the computation of six performance indices, including precision, accuracy, sensitivity, Matthews Correlation Coefficient (MCC), Cohen's kappa, and F1 score, provides a multifaceted evaluation of classifier performance, allowing for nuanced comparisons and insights into their capabilities. The computation of multiple performance indices is crucial in evaluating the effectiveness and reliability of classifiers in motion analysis. Accuracy, as a fundamental measure, indicates the overall correctness of the classifier's predictions, providing a broad assessment of its performance. Precision emphasizes the ratio of true positive predictions to all positive predictions, offering insights into the classifier's ability to

Algorithm-1 Extracting gait events, gait phases, and temporal gait parameters from the FSR signal: Benchmark data

Input:	Angular velocity from shank worn IMU signal: Gyz FSR sensor signal: FSRtoe, and FSRheel	
Output:	Gait event: HS and TO Gait Phases: Swing and Stance Temporal gait parameters: Stance period, Stride time, Swing period and Step time	
	Start	
1:	**if** ($Gyz \geq Gyz_{max}$)	// initiation of trial
2:	start=1	
3:	***while*** (start ==1)	//within the trial
4:	***if*** FSRheel==1	//check for the heel strike
5:	HS (i)=current time stamp	//record the heel strike time
6:	***if*** FSRtoe==1	//check for the toe-off
7:	TO(i)=current time stamp	//record the toe-off time
8:	***else*** wait for FSRtoe ==1	//wait for toe-off
9:	***end***	
10:	***else*** wait for FSRheel==1	//wait for heal strike
11:	***end***	
12:	***if*** ($Gyz \geq Gyz_{max}$)	//end of trial
13:	start=0;	
14:	goto step 20	
15:	***else*** goto step 4	
16:	***end***	
17:	***end***	
18:	***else*** wait ($Gyz \geq Gyz_{max}$)	//Wait for initiation of trial
19:	***end***	
20:	*Estimate all the gait temporal parameters using eq 1-4*	
	Stop	

Fig. 6. Algorithm to estimate the gait events and phases from the FSR signal. .

avoid false positives. The sensitivity of a prediction system is defined as the percentage of correct predictions relative to the total number of positive instances, highlighting the classifier's capability to detect positive cases accurately. The F1-score is a harmonic average of precision and sensitivity, balances these two metrics, and provides a comprehensive evaluation of the classifier's overall performance. Cohen's kappa statistic assesses the agreement between the classifier's predictions and the ground truth labels, considering the possibility of random agreement, thus offering a robust measure of classification reliability. Whereas the MCC provides a balanced assessment of classifier performance even in imbalanced datasets. Collectively, these performance measures offer a nuanced understanding of classifier capabilities, allowing researchers to make informed decisions regarding their suitability for motion analysis tasks [46].

The output stream of the detected gait phase from each classification method was subjected to a "postprocessing algorithm" with the objective of identifying and eliminating outliers that were embedded in larger sections that belonged to the other class. When a cluster was less than half a window (i.e., 7 samples or 0.07 s) and preceded and followed by a larger, differently categorized array, the cluster was said to be an "outlier" (Fig. 7). The current class is "preferred" by the correction process, which operates consecutively. Short clusters designated as "swing" are changed into "stance" if we are in a "stance" phase. Further, from the corrected gait phase stream, gait events were found by detecting the transitions from stance to swing (TO event) and swing to stance (HS event). This post-processing algorithm improves the proposed model performance in detecting the GPs and GEs and so as in estimating gait temporal parameters. For the presented study, the performance of three different classifiers, KNN, LDA, and SVM, were evaluated and compared for the individual subject. In addition, a machine learning toolbox in MATLAB (R2020b) was utilized to find the optimum parameters of SVM, LDA, and KNN. The optimum value of the hyperparameters of different classifiers is estimated. The complete algorithm is presented in Fig. 8.

III. Results

In the presented work, the ML model has been implemented to first evaluate the gait phases (swing, stance) and then using the phase information, the gait events (TO, HS), and temporal gait parameters has been estimated using single IMU signal. The performance of three different classifiers has been compared comprehensively for ten subjects. For each subject, a total of ten walking trials have been recorded, and from each walking trial, five gait cycles have been used for dataset preparation. The gait phase detection problem has been considered a two-class classification problem.

Table I displays the diverse evaluation metrics of the GP detection model across individual subjects and all classifiers. The % classification accuracy of the SVM classifier ranges between

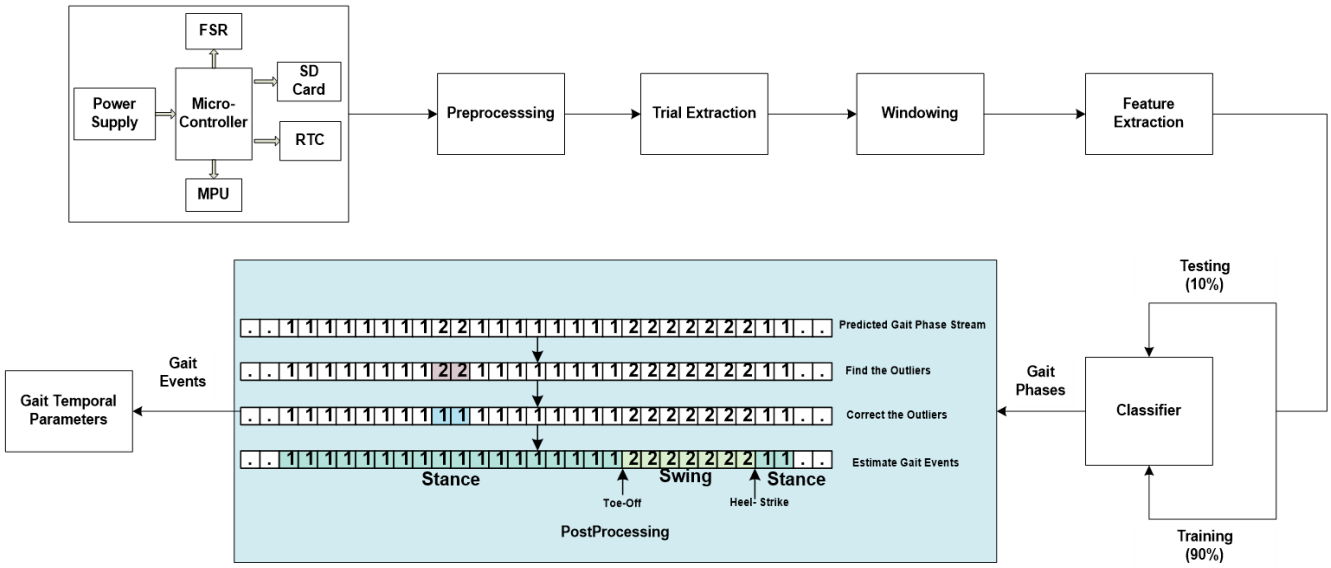

Fig. 7. Signal processing pipeline utilized for gait characterization module design using the IMU signal.

Algorithm-2 Estimating gait events, gait phases, and Temporal gait parameters from IMU signal

Input:	Acceleration and Angular velocity from shank-worn IMU signal: Accx, Accy, Accz, Gyx, Gyy and Gyz	
Output:	Gait Phases: Swing and Stance Gait event: HS and TO Temporal gait parameters: Stance period, Stride time, Swing period and Step time	
	Start	
1:	***for*** each trial	
2:	Preprocess all the signals of IMU	//Filtering
3:	***for*** *each window (window size=15 sample and window shift=1 sample)*	//Extract the signal window of 15 sample
4:	Extract the feature for the IMU signal	//A Total of six features for each signal have been extracted
5:	Construct the feature vector using all the features	//Feature will have a total of 36 features
6:	Label the feature vector *(as per the stance/swing phase)* and add to dataset	//Labelling will be done as per FSR signal
7:	***end***	
8:	***end***	
9:	Divide the dataset into subsets as per 10-fold cross-validation	//Prepare the dataset for cross-validation
10:	***for*** each subset of a dataset	//Estimate the performance of classifiers for each subset
11:	Train and test the classifiers for predicting the gait phase (stance/swing)	//Three classifiers have been compared
12:	Postprocess the predicted gait phase stream to filter the outliers	//
13:	Evaluate the performance indices	//performance indices for classifier performance
14:	Estimate the gait events (HS/TO) from the post-processed gait phase stream	
15:	Estimate all the gait temporal parameters using eq 1-4	
16:	***end***	
	Stop	

Fig. 8. Complete algorithm for temporal gait temporal parameters estimation.

80.37-99.29%, for the LDA classifier, it is between 89.63-99.26%, and for the KNN classifier, it is found between 72.20-98.73%. Whereas the average % classification accuracy has been found as 95.68±5.22%, 96.64±5.02%, and 93.62±4.83% ($p - value < 0.05$) for SVM, LDA, and KNN classifiers, respectively. The proposed model performance is equally

dependent on the correct classification of stance as well as the swing phase. Hence, to compare the performance of classifiers more comprehensively, precision, sensitivity, F1 score, C_{kappa}, and MCC are also estimated. It will provide more insight into the results obtained using the developed classification model. The average % precision has been found as 96.58±4.26, 97.72±3.81, and 96.47±3.80 ($p - value > 0.05$) for SVM, LDA, and KNN classifiers, respectively. The average % recall has been reported as 97.32±3.85, 97.45±3.99, and 94.31±4.25 ($p - value < 0.05$) for SVM, LDA, and KNN classifiers, respectively. Further, by analyzing the performance of the classifier in view of sensitivity and recall more closely F1 score has been estimated. The average % F1 score has been found as 96.91±3.78, 97.54±3.71, and 95.32±3.61 ($p - value < 0.05$) for SVM, LDA, and KNN classifiers, respectively.

The sensitivity and F1 score, all the evaluation metrics, have been found satisfactory for all the compared classifiers. The human GC consists of 60-70% of the STP and 40-30% of the SWP. There exists slight data imbalance distribution in the dataset. Hence, for all the compared classifiers C_{kappa}, and MCC have been estimated. For all the compared classifiers, the average Ckappa has been found to be greater than 86. Moreover, the average % MCC has been found as 91.07±8.92, 93.29±8.36, and 86.82±7.31 ($p - value < 0.05$) for SVM, LDA, and KNN classifiers, respectively. The LDA classifier demonstrates the highest performance among all classifiers, while the KNN exhibits the lowest performance across all performance measures compared. Therefore, when it comes to classifying phases, the LDA classifier is a more favorable choice compared to the SVM and KNN classifiers.

Fig. 9 depicts the confusion matrix of all three classifiers for gait phase classification. For SVM and LDA classifiers, the misclassification instances for both the phases (stance and swing) have been found to be at par for SVM and LDA classifiers. However, for the KNN classifier, the misclassification instances for the swing phase have been found to almost double as compared to the stance phase. It reflected the suitability of LDA and SVM over the KNN classifier for phase classification.

Fig. 10 depicts a graphical representation of the predicted GP classes and actual GP classes for one trial of subject 1. The dotted lines illustrate the predicted GP classes by the respective classifier, while solid lines represent the actual GP classes estimated by FSR sensors. It has been observed from the figure that in phase classification, two types of error can occur, outlier type (red patch) and continuous type (yellow patch). The first type of error, the outlier type, can be well eliminated during the postprocessing and will have no adverse effect on the final performance of the system. However, the second type of error, the continuous type, cannot be handled by postprocessing and remains in the system, which further reduces the performance of the system while estimating the gait temporal parameters.

Table II presents the average temporal gait parameters estimated from FSR sensors (actual value) and predicted values from the outcome of different classifiers. SVM and LDA classifiers estimated the temporal gait parameters more accurately as compared to KNN classifiers. Moreover, the variation in

SVM		TRUE	
		Stance	Swing
Predicted	Stance	69.62	1.28
	Swing	1.79	27.31

LDA		TRUE	
		Stance	Swing
Predicted	Stance	69.66	1.23
	Swing	1.05	28.05

KNN		TRUE	
		Stance	Swing
Predicted	Stance	67.82	3.08
	Swing	1.81	27.29

Fig. 9. Confusion matrix of all three classifiers for phase classification.

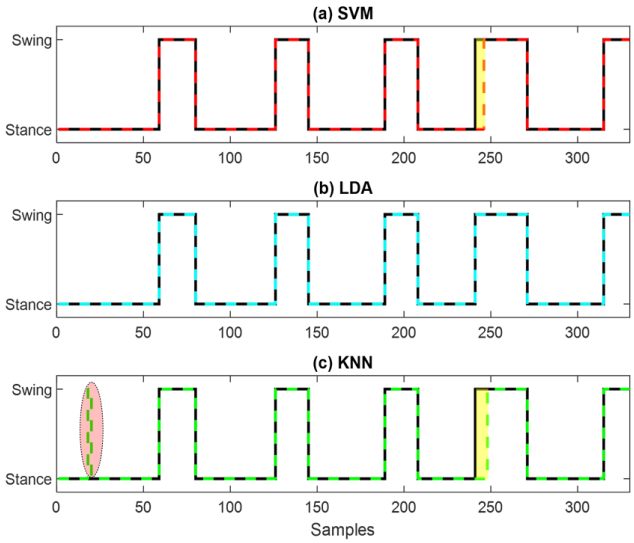

Fig. 10. Graphical representation of the predicted gait phase classes and actual gait phase classes for one trial of subject 1. (Red patch: Outlier type error, yellow patch: continuous error).

estimated parameters has been found to be minimum for the LDA classifier and maximum for the KNN classifier.

Further, to gauge the resilience of the proposed model, its performance towards the subject invariability and sensor location invariability has been evaluated. To evaluate the subject variability, the proposed model performance has been evaluated for the naive subject. Fig. 11 depicts the methodology utilized for cross-subject performance estimation. The classifier has been trained for the dataset of all the subjects, excluding the data of the subject to be tested. Fig. 12 shows the % classification accuracy of all the classifiers for gait phase detection. The performance of the KNN classifier has been significantly reduced by 3.03%, it came down to 90.78 ± 6.05% from 93.62 ± 4.83% ($p - value < 0.05$). Whereas, for SVM, it has been reduced by 2.30% and estimated as 93.48 ± 6.84% ($p - value > 0.05$). The best performance is shown by the LDA classifier as 95.52 ± 5.18%. with a reduction of only 1.15% ($p - value > 0.05$).

Further,the proposed model performance for different sensor locations has been estimated for its robustness towards sensor location variability. Fig. 13 depicts the different sensor locations used for signal acquisition. Initially, the data acquisition of ten subjects was done by keeping the sensor at location-1 (just above the ankle). However, to further test the sensor location variability on model performance, the data has also been acquired by positioning the sensor at location 2 (in the middle of the shank) and location 3 (just below the knee) separately. The classifiers have been trained with the dataset of location-1 and tested for datasets of both location-2 and

TABLE I
PERFORMANCE OF DIFFERENT CLASSIFIERS FOR GAIT PHASE DETECTION

SVM						
Subject No.	**Accuracy**	**Precision**	**Sensitivity**	**F1 score**	C_{kappa}	**MCC**
S1	91.37 ± 18.14	93.27 ± 12.30	94.36 ± 14.46	93.71 ± 13.21	87.34 ± 19.96	89.07 ± 15.75
S2	97.61 ± 3.44	97.12 ± 5.05	99.57 ± 0.88	98.26 ± 2.64	94.28 ± 7.59	94.66 ± 6.92
S3	98.82 ± 2.11	99.26 ± 1.03	99.23 ± 1.82	99.24 ± 1.29	96.44 ± 7.15	96.49 ± 7.06
S4	98.11 ± 2.55	98.06 ± 3.10	99.23 ± 1.21	98.62 ± 1.87	95.66 ± 5.85	95.78 ± 5.59
S5	97.93 ± 2.69	98.66 ± 0.88	98.53 ± 3.57	98.56 ± 1.88	94.89 ± 6.54	95.09 ± 6.06
S6	97.92 ± 1.88	97.81 ± 2.84	99.23 ± 1.15	98.49 ± 1.39	95.17 ± 4.28	95.33 ± 4.04
S7	98.19 ± 1.67	99.08 ± 1.22	98.31 ± 2.02	98.68 ± 1.23	95.79 ± 3.83	95.86 ± 3.77
S8	80.37 ± 14.88	85.68 ± 11.12	86.63 ± 11.18	86.08 ± 10.80	55.65 ± 29.02	56.34 ± 28.86
S9	97.29 ± 3.51	97.68 ± 3.82	98.47 ± 1.44	98.04 ± 2.49	93.64 ± 8.39	93.76 ± 8.15
S10	99.29 ± 1.39	99.24 ± 1.31	99.71 ± 0.88	99.47 ± 1.07	98.40 ± 3.04	98.41 ± 3.04
LDA						
Subject No.	**Accuracy**	**Precision**	**Sensitivity**	**F1 score**	C_{kappa}	**MCC**
S1	91.24 ± 20.60	93.74 ± 14.01	93.13 ± 17.61	93.30 ± 15.90	89.12 ± 19.36	91.29 ± 13.58
S2	96.68 ± 4.03	96.24 ± 5.41	98.83 ± 1.86	97.44 ± 3.20	92.74 ± 8.58	93.04 ± 8.13
S3	99.26 ± 1.99	99.67 ± 0.69	99.42 ± 1.75	99.54 ± 1.21	97.58 ± 6.67	97.62 ± 6.55
S4	98.42 ± 2.15	98.53 ± 2.60	99.23 ± 1.37	98.86 ± 1.52	96.29 ± 5.18	96.42 ± 4.91
S5	99.12 ± 2.05	99.75 ± 47	99.09 ± 2.74	99.40 ± 1.41	97.77 ± 5.12	97.90 ± 4.75
S6	98.91 ± 1.18	99.42 ± 0.76	99.02 ± 1.40	99.22 ± 0.82	97.42 ± 2.97	97.46 ± 2.91
S7	98.76 ± 1.76	99.54 ± 0.87	98.66 ± 2.06	99.09 ± 1.29	97.15 ± 4.06	97.20 ± 3.99
S8	89.63 ± 9.65	94.09 ± 7.35	91.37 ± 7.21	92.66 ± 6.94	74.81 ± 22.96	75.13 ± 23.04
S9	96.01 ± 4.57	96.86 ± 5.09	97.53 ± 1.48	97.15 ± 3.24	90.52 ± 10.89	90.72 ± 10.57
S10	98.36 ± 2.38	99.37 ± 0.90	98.29 ± 2.46	98.82 ± 1.66	96.13 ± 5.34	96.18 ± 5.25
KNN						
Subject No.	**Accuracy**	**Precision**	**Sensitivity**	**F1 score**	C_{kappa}	**MCC**
S1	87.97 ± 18.13	92.11 ± 12.61	90.35 ± 14.89	91.11 ± 13.67	79.87 ± 17.23	81.75 ± 12.70
S2	98.25 ± 2.62	98.71 ± 2.77	98.83 ± 1.33	98.75 ± 1.87	95.84 ± 6.26	95.91 ± 6.13
S3	97.62 ± 2.77	98.97 ± 1.03	97.87 ± 2.79	98.40 ± 1.79	93.47 ± 8.38	93.61 ± 8.11
S4	96.09 ± 3.27	98.39 ± 3.13	95.79 ± 2.22	97.06 ± 2.51	91.21 ± 7.23	91.33 ± 7.24
S5	96.10 ± 4.05	98.82 ± 0.89	95.78 ± 5.15	97.21 ± 2.94	90.72 ± 9.23	91.12 ± 8.35
S6	94.53 ± 1.67	97.71 ± 3.34	94.39 ± 3.0	95.93 ± 1.29	87.57 ± 3.65	88.05 ± 3.35
S7	97.41 ± 1.23	98.74 ± 1.89	97.58 ± 1.28	98.14 ± 0.89	93.82 ± 2.96	93.94 ± 2.90
S8	72.20 ± 11.97	82.96 ± 10.15	76.50 ± 8.89	79.54 ± 9.18	40.58 ± 18.51	41.41 ± 18.34
S9	97.38 ± 1.51	98.70 ± 1.29	97.50 ± 1.84	98.09 ± 1.08	93.94 ± 3.56	94.02 ± 3.50
S10	98.73 ± 1.17	99.60 ± 0.90	98.54 ± 1.19	99.06 ± 0.91	97.04 ± 2.52	97.07 ± 2.51

TABLE II
AVERAGE TEMPORAL GAIT PARAMETERS

Gait Parameters	**Actual (FSR)**	**SVM**	**LDA**	**KNN**
Stride Time (sec)	0.87 ± 0.11	0.88 ± 0.12	0.88 ± 0.10	0.89 ± 0.09
Stance Time (sec)	0.62 ± 0.02	0.62 ± 0.03	0.62 ± 0.02	0.63 ± 0.08
Swing Time (sec)	0.26 ± 0.04	0.26 ±0.04	0.26 ± 0.05	0.27 ± 0.02
Step Time (sec)	0.43 ± 0.05	0.43 ± 0.05	0.44 ± 0.05	0.44 ± 0.04

location-3 individually. Fig. 14 shows the % classification accuracy of classifiers when the classifier has been trained with a dataset of sensors at location-1 and tested with the dataset of sensors at location-1, location-2, and location-3 separately. The performance of SVM and LDA classifiers has been found consistent for all sensor locations ($p - value > 0.05$). However, for the KNN classifier, a slight reduction in performance has been observed ($p - value < 0.05$)

Table III presents a comparison of existing techniques and the proposed model in this study. The proposed model performance has been found to be better over all the compared performance indices. Moreover, the proposed model performance has also been found to be invariant to the different sensor placement locations, which is not the case with existing techniques.

TABLE III
COMPARISON OF THE PROPOSED METHOD WITH OTHER EXISTING METHODS

Authors	**Method**	**Accuracy**	**Precision**	**Recall**	**F1-Score**
Zhang et al. [47]	SVM	87.87%	94.96%	90.74%	91.53%
Attal et al. [48]	MRHMM	84.64%	85.00%	84.05%	84.38%
Liu et al. [49]	HMM	91.88%	91.58%	90.50%	90.95%
Tiwari et al. [50]	CNN	83.45%	-	-	-
Liu et al. [51]	LMM	96.00%	-	-	-
Panahandeh et al. [52]	HMM	95.00%	-	-	-
Dehzangi et al. [53]	CNN	91%	-	-	-
Gadaleta et al. [54]	CNN	80%	-	-	-
Rampp et al. [55]	LSTM	90%	-	-	-
Proposed Method	**LDA**	**96.64%**	**97.72%**	**97.45%**	**97.54%**

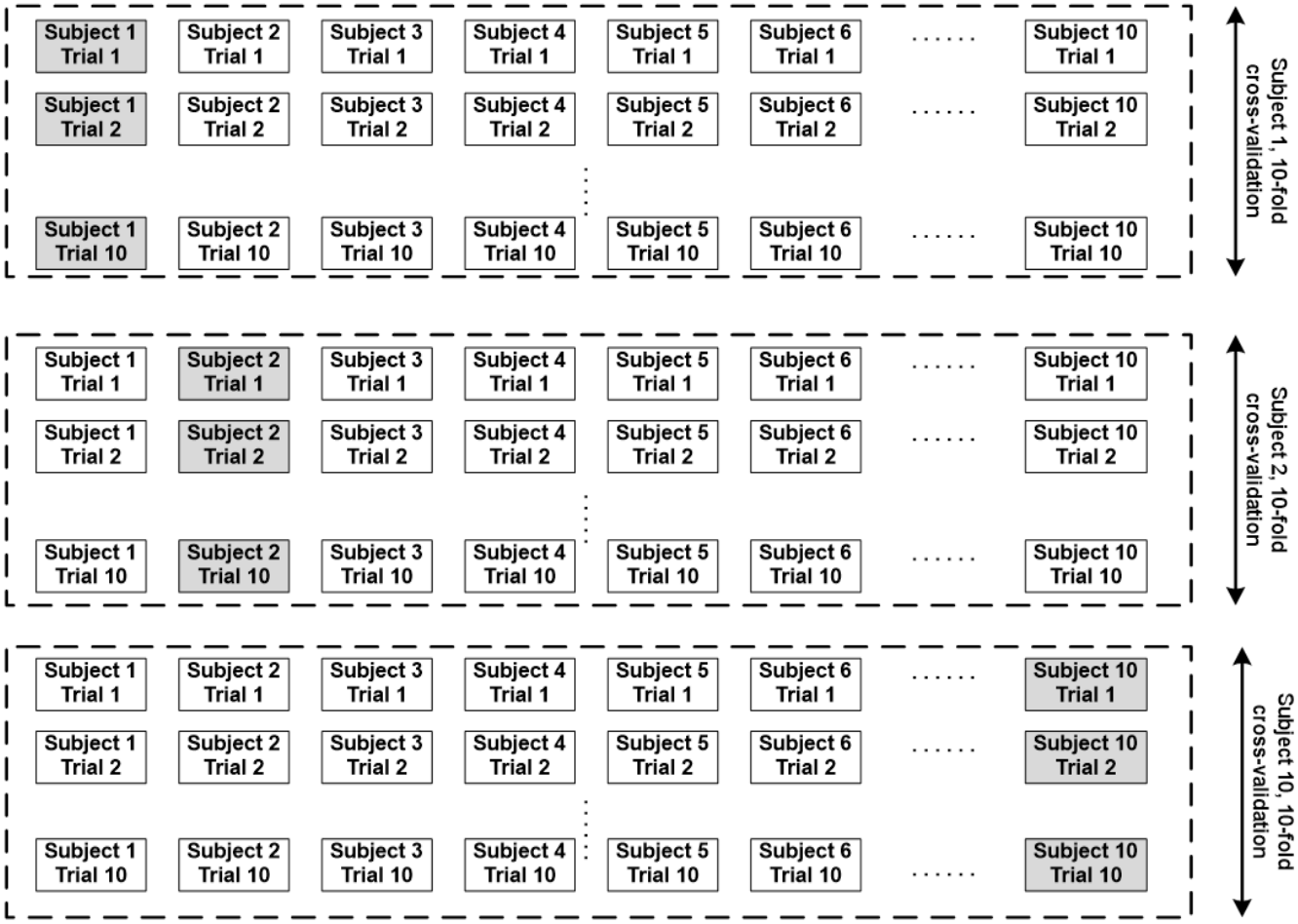

Fig. 11. Methodology for cross-subject performance estimation (Gray box depicts the data used to test the classifier).

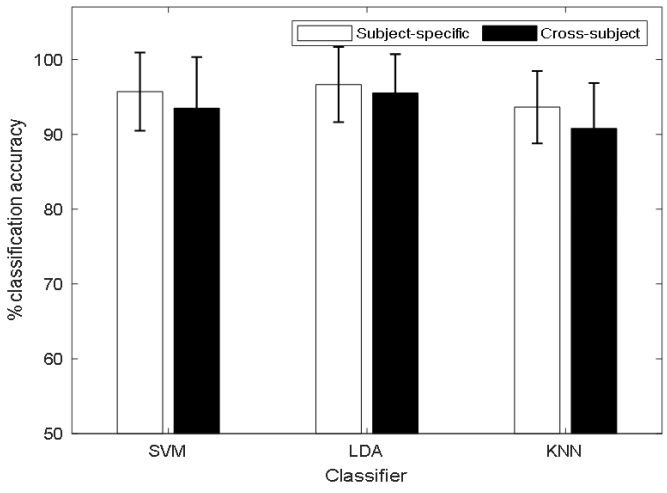

Fig. 12. Subject-specific and cross-subject performance of classifiers for gait phase classification.

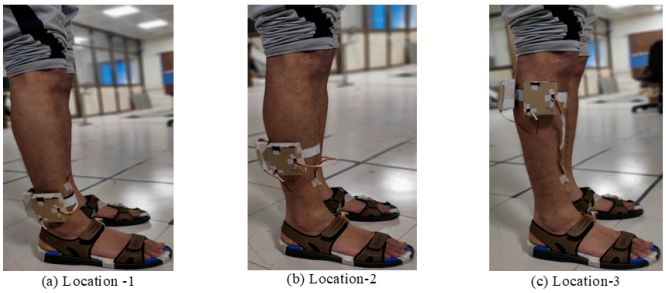

Fig. 13. Different sensor placement locations.

IV. Discussion

The gait phase, gait event, and its temporal information play a very vital role in rehabilitation, predicting neuromuscular disorder, sleep disorder, exoskeleton, and prosthesis control. However, the existing methods are expensive, highly dependent on a controlled environment, and require a higher number of sensors. The primary contribution of this study was to devise a portable, cost-effective system utilizing a single IMU sensor and ML for gait parameter estimation. This system aims to detect gait phases, gait events, and estimate gait temporal parameters. The developed hardware module consists of 6 DoF single-IMU sensors, a microcontroller, an SD card interface, and a power supply module. Moreover, a modular insole with four FSR sensors has also been designed and interfaced with the developed module. The signal recorded with the insole

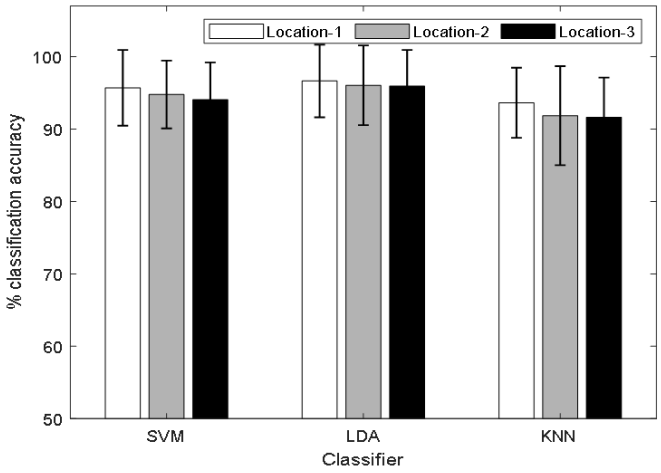

Fig. 14. Classifier performance trained with data of sensor at location-1 and tested with different sensor locations.

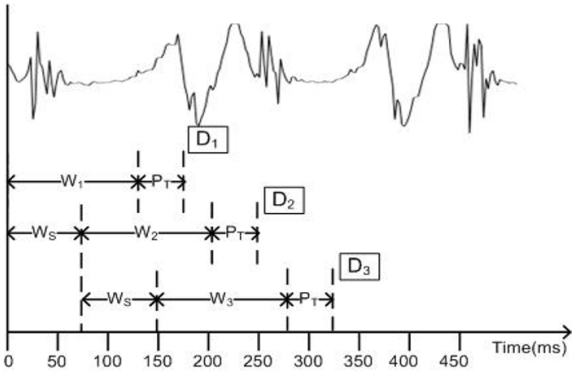

Fig. 15. Continuous overlapping windowing.

has been used to test and validate the performance of the IMU-based system regarding the GP, GE, and gait temporal parameter estimation. The developed hardware is portable, user-friendly, easy to wear, position invariant, calibration-free, suitable for outdoor use, and consumes 100 mA current when running at full speed of 600 MHz and operates on 1.25 V.

The overall study was conducted on ten participants with their self-paced walking speed. A ML approach has been proposed to continuously predict the gait phase, and gait events, and evaluate temporal gait parameters. Moreover, a postprocessing strategy has also been proposed and validated to filter out the gait phase outliers from the classification results. To validate the efficacy of the proposed method, the performance of three different classifiers has been compared based on six performance indices. The continuous prediction feature has been incorporated into the developed model by implementing an overlapping windowing technique which makes it more suitable for real-time applications. Fig. 15 illustrates the overlapping windowing technique with its time complexity. As shown in Figure, W1, W2, and W3 are successive windows. For each window, the classification decision (D1, D2, and D3) is made PT seconds later, where PT is the processing time, including the time taken for the feature vector preparation and decision-making by the classifier. The window length specifies the quantity of data utilized for feature extraction and classification, resulting in a single decision. The step size of the sliding window WS controls the response time of the system between two decisions. Moreover, the processing time PT of the system should be less than or equal to the step size of the sliding window to fully utilize the computing capacity of the developed system. In this study, the window length and window shift has been kept as 15 samples (150 ms) and 1 sample (10 ms), respectively. So, in faithful real-time implementation, the processing time should be less than or equal to 10 ms. The average processing time for SVM, LDA, and KNN classifiers are found to be 0.0046±0.0232 sec, 0.0023±0.0046 sec, and 0.0044±0.0300 sec respectively. The time delay generated due to the processing time is quite low hence it does not impact the decisions of the proposed system. Here, to predict the GP, the signal of only a single IMU sensor has been utilized, which eliminates the synchronization issue related to multiple sensors. For each window of the IMU signal, time domain features have been estimated and concatenated to prepare the feature vector. The proposed methodology is suitable for real-time embedded implementation as it utilizes the continuous overlapping windowing technique, single IMU sensor, and time domain features.

The proposed GE detection methodology utilized the GP classification model to predict the GE, i.e., first, the gait phase has been predicted, and then the gait events are estimated. Further, there are two types of possible errors that have been observed in the gait phase classification, the outlier type, and the continuous type, as shown in Figure 10. A postprocessing technique has also been proposed and implemented to remove the outlier type error in gait phase detection. In the current study, we have observed seven continuous gait phase classification results. However, it can be tuned by the developer to achieve the best results. The proposed postprocessing technique makes the gait event detection more immune to such type of error, which can also be generated due to involuntary foot movement, foot tapping by post-stroke patients [28], subjects suffering from Parkinson's, or any other neuromuscular disorders [56], [57].

The performance for gait phase prediction has been estimated for SVM, LDA, and KNN classifiers. The average % classification accuracy over ten subjects has been found to be 95.68±5.22%, 96.64±5.02%, and 93.62±4.83% ($p - value < 0.05$) for SVM, LDA, and KNN classifiers, respectively. Further, to compare the performance of three classifiers, five more performance measures (precision, sensitivity, F1 score, C_{kappa}, and MCC) have been estimated and compared. The C_{kappa}, and MCC performance measures justify the efficacy of the proposed model over the imbalanced dataset. Further, the gait temporal parameters are estimated satisfactorily. The LDA classifier depicts the minimum variation in temporal gait parameter estimation as compared to SVM and KNN classifiers. Based on all estimated performance measures LDA classifier outperformed SVM and KNN classifiers. Furthermore, the proposed model performance has been estimated for subject variation and sensor location variation. In the case

of subject variation estimation, the model has been tested for a naive subject. LDA classifier depicted the minimum change in performance, whereas KNN depicted the maximum.

The performance of the developed module suggests that it can be used by the wide population directly without any subject-specific training. The effect of sensor placement location has also been estimated for three different sensor positions. The proposed model performance has been found to be consistent for all the sensor locations, which makes it user-friendly and robust. However, there are some limitations of the developed model which could be covered in future studies. One of the limitations of the presented study is that the proposed method is validated only on the healthy population with their self-selected walking speed on a single type of terrain. In the next phase of work, the proposed method could be implemented on an embedded system, and its long-term continuous performance could be evaluated over a variety of populations in an unconstrained environment.

V. Conclusion

Human gait characterization helps in the treatment and rehabilitation of people with movement/neurodevelopmental disorders. Early assessment of the problem can help in diagnosing/predicting neuromotor disorders at primary stages. However, the current approach for diagnosis is confined to a sophisticated and controlled instrumentation laboratory, which is out of the reach for a large population. The gait characterization module should be user-friendly, cost-effective, robust, and efficient. In the present research work, a machine learning-based wearable sensor module has been developed, that consists of only a single IMU sensor. The LDA classifier showed the best classification accuracy for gait phase prediction as 96.64±5.02% ($p - value < 0.05$), in comparison to SVM and KNN classifiers. Further, a post-processing algorithm has been proposed to estimate the gait events from the predicted gait phases. The temporal gait parameters have also been estimated from the series of gait events. Stance and swing time measured using the LDA classifier have been found very close to reference values ($p - value > 0.05$) as 0.62 ± 0.02 and 0.26 ± 0.05 (sec), respectively. Moreover, the robustness of the proposed model is validated with changing sensor location as well as recruiting naive subjects to predict the gait phase accurately. The results obtained from this study will help the therapist in the treatment, management and rehabilitation of gait associated neurological disorders. In future, an integrated embedded system powered by deep learning models will be developed for the on-site and off-site implementation of the technology for the telemedicine-based diagnosis, rehabilitation and management of movement related disorders.

Acknowledgments

The authors extend their heartfelt gratitude to the esteemed members of the Neurocomputing Lab IITD for their invaluable support throughout this project. Additionally, the authors would like to thank the volunteers whose dedicated contributions greatly facilitated the data collection process.

References

[1] R. Baker, "Gait analysis methods in rehabilitation," *Journal of neuroengineering and rehabilitation*, vol. 3, pp. 1–10, 2006.

[2] S. T. Moore, H. G. MacDougall, and W. G. Ondo, "Ambulatory monitoring of freezing of gait in parkinson's disease," *Journal of neuroscience methods*, vol. 167, no. 2, pp. 340–348, 2008.

[3] A. Salarian, H. Russmann, F. J. Vingerhoets, P. R. Burkhard, and K. Aminian, "Ambulatory monitoring of physical activities in patients with parkinson's disease," *IEEE Transactions on Biomedical Engineering*, vol. 54, no. 12, pp. 2296–2299, 2007.

[4] H. F. Maqbool, M. A. B. Husman, M. I. Awad, A. Abouhossein, N. Iqbal, M. Tahir, and A. A. Dehghani-Sanij, "Heuristic real-time detection of temporal gait events for lower limb amputees," *IEEE Sensors Journal*, vol. 19, no. 8, pp. 3138–3148, 2018.

[5] S. Lahmiri, "Gait nonlinear patterns related to parkinson's disease and age," *IEEE Transactions on Instrumentation and Measurement*, vol. 68, no. 7, pp. 2545–2551, 2018.

[6] V. Mikos, C.-H. Heng, A. Tay, S.-C. Yen, N. S. Y. Chia, K. M. L. Koh, D. M. L. Tan, and W. L. Au, "A wearable, patient-adaptive freezing of gait detection system for biofeedback cueing in parkinson's disease," *IEEE transactions on biomedical circuits and systems*, vol. 13, no. 3, pp. 503–515, 2019.

[7] A. Prado, S. K. Kwei, N. Vanegas-Arroyave, and S. K. Agrawal, "Continuous identification of freezing of gait in parkinson's patients using artificial neural networks and instrumented shoes," *IEEE Transactions on Medical Robotics and Bionics*, vol. 3, no. 3, pp. 554–562, 2021.

[8] K. Turcot, R. Aissaoui, K. Boivin, M. Pelletier, N. Hagemeister, and J. A. de Guise, "New accelerometric method to discriminate between asymptomatic subjects and patients with medial knee osteoarthritis during 3-d gait," *IEEE Transactions on Biomedical Engineering*, vol. 55, no. 4, pp. 1415–1422, 2008.

[9] Y. Hutabarat, D. Owaki, and M. Hayashibe, "Quantitative gait assessment with feature-rich diversity using two imu sensors," *IEEE Transactions on Medical Robotics and Bionics*, vol. 2, no. 4, pp. 639–648, 2020.

[10] Y. Wahab and N. A. Bakar, "Gait analysis measurement for sport application based on ultrasonic system," in *2011 IEEE 15th international symposium on consumer electronics (ISCE)*. IEEE, 2011, pp. 20–24.

[11] M. Zhang, D. Liu, Q. Wang, B. Zhao, O. Bai, and J. Sun, "Gait pattern recognition based on plantar pressure signals and acceleration signals," *IEEE Transactions on Instrumentation and Measurement*, vol. 71, pp. 1–15, 2022.

[12] K. Watanabe and M. Hokari, "Kinematical analysis and measurement of sports form," *IEEE Transactions on Systems, Man, and Cybernetics-Part A: Systems and Humans*, vol. 36, no. 3, pp. 549–557, 2006.

[13] D. Solanki and U. Lahiri, "Design of instrumented shoes for gait characterization: A usability study with healthy and post-stroke hemiplegic individuals," *Frontiers in neuroscience*, vol. 12, p. 459, 2018.

[14] B. Toro, C. Nester, and P. Farren, "A review of observational gait assessment in clinical practice," *Physiotherapy theory and practice*, vol. 19, no. 3, pp. 137–149, 2003.

[15] A. Cappozzo, U. Della Croce, A. Leardini, and L. Chiari, "Human movement analysis using stereophotogrammetry: Part 1: theoretical background," *Gait & posture*, vol. 21, no. 2, pp. 186–196, 2005.

[16] A. Muro-De-La-Herran, B. Garcia-Zapirain, and A. Mendez-Zorrilla, "Gait analysis methods: An overview of wearable and non-wearable systems, highlighting clinical applications," *Sensors*, vol. 14, no. 2, pp. 3362–3394, 2014.

[17] F. Wang, E. Stone, W. Dai, M. Skubic, and J. Keller, "Gait analysis and validation using voxel data," in *2009 Annual International Conference of the IEEE Engineering in Medicine and Biology Society*. IEEE, 2009, pp. 6127–6130.

[18] W. Tao, T. Liu, R. Zheng, and H. Feng, "Gait analysis using wearable sensors," *Sensors*, vol. 12, no. 2, pp. 2255–2283, 2012.

[19] A. S. Alharthi, A. J. Casson, and K. B. Ozanyan, "Gait spatiotemporal signal analysis for parkinson's disease detection and severity rating," *IEEE Sensors Journal*, vol. 21, no. 2, pp. 1838–1848, 2020.

[20] E. Sardini, M. Serpelloni, and M. Lancini, "Wireless instrumented crutches for force and movement measurements for gait monitoring," *IEEE Transactions on Instrumentation and Measurement*, vol. 64, no. 12, pp. 3369–3379, 2015.

[21] J. Lecoutere, A. Thielens, S. Agneessens, H. Rogier, W. Joseph, and R. Puers, "Wireless fidelity electromagnetic field exposure monitoring with wearable body sensor networks," *IEEE transactions on biomedical circuits and systems*, vol. 10, no. 3, pp. 779–786, 2015.

[22] P. Parik-Americano, J. P. Pinho, F. C. dos Santos, G. S. Umemura, L. R. Battistella, and A. Forner-Cordero, "Lower limb exoskeleton during gait and posture: Objective and subjective assessment procedures with minimal instrumentation," *IEEE Transactions on Medical Robotics and Bionics*, 2023.

[23] O. Beauchet, F. R. Herrmann, R. Grandjean, V. Dubost, and G. Allali, "Concurrent validity of smtec® footswitches system for the measurement of temporal gait parameters," *Gait & posture*, vol. 27, no. 1, pp. 156–159, 2008.

[24] M. Chen, B. Huang, and Y. Xu, "Intelligent shoes for abnormal gait detection," in *2008 IEEE international conference on robotics and automation*. IEEE, 2008, pp. 2019–2024.

[25] J. Pawin, T. Khaorapapong, and S. Chawalit, "Neural-based human's abnormal gait detection using force sensitive resistors," in *The Fourth International Workshop on Advanced Computational Intelligence*. IEEE, 2011, pp. 224–229.

[26] A. J. A. Majumder, S. I. Ahamed, R. J. Povinelli, C. P. Tamma, and R. O. Smith, "A novel wireless system to monitor gait using smartshoe-worn sensors," in *2015 IEEE 39th Annual Computer Software and Applications Conference*, vol. 2. IEEE, 2015, pp. 733–741.

[27] S. Perry and M. Lafortune, "Influences of inversion/eversion of the foot upon impact loading during locomotion," *Clinical Biomechanics*, vol. 10, no. 5, pp. 253–257, 1995.

[28] S. Yang, J.-T. Zhang, A. C. Novak, B. Brouwer, and Q. Li, "Estimation of spatio-temporal parameters for post-stroke hemiparetic gait using inertial sensors," *Gait & posture*, vol. 37, no. 3, pp. 354–358, 2013.

[29] S. P. Rana, M. Dey, M. Ghavami, and S. Dudley, "3-d gait abnormality detection employing contactless ir-uwb sensing phenomenon," *IEEE Transactions on Instrumentation and Measurement*, vol. 70, pp. 1–10, 2021.

[30] L. Zhou, E. Fischer, C. Tunca, C. M. Brahms, C. Ersoy, U. Granacher, and B. Arnrich, "How we found our imu: Guidelines to imu selection and a comparison of seven imus for pervasive healthcare applications," *Sensors*, vol. 20, no. 15, p. 4090, 2020.

[31] C.-C. Yang and Y.-L. Hsu, "A review of accelerometry-based wearable motion detectors for physical activity monitoring," *Sensors*, vol. 10, no. 8, pp. 7772–7788, 2010.

[32] P. Fraccaro, L. Coyle, J. Doyle, and D. O'Sullivan, "Real-world gyroscope-based gait event detection and gait feature extraction," 2014.

[33] F. A. Garcia, J. C. Pérez-Ibarra, M. H. Terra, and A. A. Siqueira, "Adaptive algorithm for gait segmentation using a single imu in the thigh pocket," *IEEE Sensors Journal*, vol. 22, no. 13, pp. 13 251–13 261, 2022.

[34] K. Ren, Z. Chen, Y. Ling, and J. Zhao, "Recognition of freezing of gait in parkinson's disease based on combined wearable sensors," *BMC neurology*, vol. 22, no. 1, pp. 1–13, 2022.

[35] C. Tunca, N. Pehlivan, N. Ak, B. Arnrich, G. Salur, and C. Ersoy, "Inertial sensor-based robust gait analysis in non-hospital settings for neurological disorders," *Sensors*, vol. 17, no. 4, p. 825, 2017.

[36] I. H. Lopez-Nava and A. Munoz-Melendez, "Wearable inertial sensors for human motion analysis: A review," *IEEE Sensors Journal*, vol. 16, no. 22, pp. 7821–7834, 2016.

[37] L.-F. Shi, H. Liu, G.-X. Liu, and F. Zheng, "Body topology recognition and gait detection algorithms with nine-axial immu," *IEEE transactions on instrumentation and measurement*, vol. 69, no. 3, pp. 721–728, 2019.

[38] H. Zhang, Y. Guo, and D. Zanotto, "Accurate ambulatory gait analysis in walking and running using machine learning models," *IEEE Transactions on Neural Systems and Rehabilitation Engineering*, vol. 28, no. 1, pp. 191–202, 2019.

[39] C.-W. Tan and S. Park, "Design of accelerometer-based inertial navigation systems," *IEEE Transactions on Instrumentation and Measurement*, vol. 54, no. 6, pp. 2520–2530, 2005.

[40] A. M. Sabatini, C. Martelloni, S. Scapellato, and F. Cavallo, "Assessment of walking features from foot inertial sensing," *IEEE Transactions on biomedical engineering*, vol. 52, no. 3, pp. 486–494, 2005.

[41] J. Hannink, T. Kautz, C. F. Pasluosta, J. Barth, S. Schülein, K.-G. Gaßmann, J. Klucken, and B. M. Eskofier, "Mobile stride length estimation with deep convolutional neural networks," *IEEE journal of biomedical and health informatics*, vol. 22, no. 2, pp. 354–362, 2017.

[42] T. Gujarathi and K. Bhole, "Gait analysis using imu sensor," in *2019 10th International Conference on Computing, Communication and Networking Technologies (ICCCNT)*. IEEE, 2019, pp. 1–5.

[43] A. Bhongade, R. Gupta, and T. K. Gandhi, "Machine learning-based gait characterization using single imu sensor," in *2022 International Conference on Computing, Communication, and Intelligent Systems (ICCCIS)*. IEEE, 2022, pp. 263–266.

[44] A. Phinyomark, P. Phukpattaranont, and C. Limsakul, "Feature reduction and selection for emg signal classification," *Expert systems with applications*, vol. 39, no. 8, pp. 7420–7431, 2012.

[45] M. Zago, M. Tarabini, M. Delfino Spiga, C. Ferrario, F. Bertozzi, C. Sforza, and M. Galli, "Machine-learning based determination of gait events from foot-mounted inertial units," *Sensors*, vol. 21, no. 3, p. 839, 2021.

[46] L.-F. Shi, C.-X. Qiu, D.-J. Xin, and G.-X. Liu, "Gait recognition via random forests based on wearable inertial measurement unit," *Journal of Ambient Intelligence and Humanized Computing*, vol. 11, pp. 5329–5340, 2020.

[47] M. Zhang, Q. Wang, D. Liu, B. Zhao, J. Tang, and J. Sun, "Real-time gait phase recognition based on time domain features of multi-mems inertial sensors," *IEEE Transactions on Instrumentation and Measurement*, vol. 70, pp. 1–12, 2021.

[48] F. Attal, Y. Amirat, A. Chibani, and S. Mohammed, "Automatic recognition of gait phases using a multiple-regression hidden markov model," *IEEE/ASME Transactions on Mechatronics*, vol. 23, no. 4, pp. 1597–1607, 2018.

[49] L. Liu, H. Wang, H. Li, J. Liu, S. Qiu, H. Zhao, and X. Guo, "Ambulatory human gait phase detection using wearable inertial sensors and hidden markov model," *Sensors*, vol. 21, no. 4, p. 1347, 2021.

[50] A. Tiwari, A. Pai, and D. Joshi, "A shoe-mounted infrared sensor-based instrumentation for locomotion identification using machine learning methods," *Measurement*, vol. 168, p. 108458, 2021.

[51] X. Liu, S. Zhang, B. Yao, Y. Yu, Y. Wang, and J. Fan, "Gait phase detection based on inertial measurement unit and force-sensitive resistors embedded in a shoe," *Review of Scientific Instruments*, vol. 92, no. 8, 2021.

[52] G. Panahandeh, N. Mohammadiha, A. Leijon, and P. Händel, "Continuous hidden markov model for pedestrian activity classification and gait analysis," *IEEE Transactions on Instrumentation and Measurement*, vol. 62, no. 5, pp. 1073–1083, 2013.

[53] O. Dehzangi, M. Taherisadr, and R. ChangalVala, "Imu-based gait recognition using convolutional neural networks and multi-sensor fusion," *Sensors*, vol. 17, no. 12, p. 2735, 2017.

[54] M. Gadaleta, L. Merelli, and M. Rossi, "Human authentication from ankle motion data using convolutional neural networks," in *2016 IEEE Statistical Signal Processing Workshop (SSP)*. IEEE, 2016, pp. 1–5.

[55] A. Rampp, J. Barth, S. Schülein, K.-G. Gaßmann, J. Klucken, and B. M. Eskofier, "Inertial sensor-based stride parameter calculation from gait sequences in geriatric patients," *IEEE transactions on biomedical engineering*, vol. 62, no. 4, pp. 1089–1097, 2014.

[56] Y. Watanabe and M. Kimura, "Gait identification and authentication using lstm based on 3-axis accelerations of smartphone," *Procedia Computer Science*, vol. 176, pp. 3873–3880, 2020.

[57] P. Pierleoni, A. Belli, O. Bazgir, L. Maurizi, M. Paniccia, and L. Palma, "A smart inertial system for 24h monitoring and classification of tremor and freezing of gait in parkinson's disease," *IEEE Sensors Journal*, vol. 19, no. 23, pp. 11 612–11 623, 2019.